O- AND H-ISOTOPE STUDY OF THE CARBON LEADER REEF AT THE TAU TONA AND SAVUKA MINES (WESTERN DEEP LEVELS), SOUTH AFRICA: IMPLICATIONS FOR THE ORIGIN AND EVOLUTION OF WITWATERSRAND BASIN FLUIDS

D. GROVÉ
Department of Geological Sciences, University of Cape Town, Rondebosch 7701, South Africa
Present address: Kopanang Mine, AngloGold Ashanti Limited
email: dgrove@AngloGoldAshanti.com

C. HARRIS
Department of Geological Sciences, University of Cape Town, Rondebosch 7701, South Africa
email: chris.harris@uct.ac.za

ABSTRACT

The Carbon Leader Reef is a ~1 m thick conglomeratic unit with a thin bituminous base, and is one of the major gold-bearing conglomerate horizons in the Central Rand Group of the Witwatersrand Basin. It consists of alternating conglomerate and quartzite layers and was metamorphosed under greenschist facies conditions. Bulk rock $\delta^{18}O$ and δD values of the Carbon Leader Reef range from 7.2‰ to 10.8‰ (mean = 10.6‰) and -27 to -65 (mean = -41‰), respectively. The narrow range in $\delta^{18}O$ values, together with the lack of correlation between the $\delta^{18}O$ value and the modal % matrix minerals, suggests that the original detrital minerals and the authigenic matrix minerals have similar oxygen isotope composition.

Calculated δD values of the fluid, assuming that it was in isotope equilibrium with the bulk rock at the estimated peak metamorphic temperature of 350°C, range from -1‰ to -40‰. This suggests that the ultimate origin of the fluid was a mixture of meteoric and metamorphic water. These data are not consistent with the ingress of large quantities of externally derived fluid post burial metamorphism. Gold-rich sections of the Carbon Leader Reef do not have significantly different $\delta^{18}O$ values than the adjacent gold-poor section, which suggests that gold mineralization is not related to interaction with significant amounts of externally derived hydrothermal fluids.

Introduction

The Late Archaean Witwatersrand basin in South Africa has yielded more than 40% of all gold mined in recorded history and a total of 48,670 metric tons were extracted between 1886 and 2000 (Frimmel and Minter, 2002). The origin of the gold has been the topic of intense debate for many years (see summary in. Frimmel, 2008) resulting in three different models that have been used to explain the mineralization.

1. The placer model: This suggests that the gold originated from an older granite-greenstone source and was deposited by fluvial/deltaic processes (e.g. Mellor, 1961; Pretorius, 1974; Hallbauer and Utter 1977).
2. The modified placer: This model is similar to the placer model, but gold concentration is presumed to have been enhanced along certain horizons by dissolution, transport and redeposition by hydrothermal fluids (e.g. Frimmel and Gartz, 1997; Frimmel, 2008).
3. The metamorphic/hydrothermal model: This suggests that gold was introduced to the basin by hydrothermal fluids that originated from outside the basin (e.g. Graton, 1930; Phillips et al., 1990; Phillips and Law 1994; Barnicoat et al., 1997).

Despite the many years of debate concerning the placer vs. hydrothermal model for the Witwatersrand gold mineralization, and despite their suitability for such investigations, only a few studies on O- and H-isotope geochemistry of the Witwatersrand Supergroup rocks have been made (Harris and Watkins, 1990; Barton et al., 1992; Vennemann et al., 1992; 1995; Zhao et al., 2006). These studies have concentrated mainly on the upper conglomerates of the Central Rand Group and in particular the Ventersdorp Contact Reef and very little data exist for the lower conglomerates of the West Rand Group. This study, at TauTona and Savuka Mines (both in the area formally known as Western Deep Levels), is the first detailed O- and H-isotope study of a single gold reef.

Notwithstanding the apparent relationship of gold distribution with sedimentary features in the Witwatersrand, the distribution of gold is also structurally controlled and is evident in scales ranging from millimetres to kilometres (e.g. Barnicoat et al., 1997; Jolley et al., 2004). This has led to the suggestion that large quantities of gold are dissolved by fluids during redistribution and mineralization. The gold mineralization in the Carbon Leader Reef, at the base of the Main Formation in the Central Rand Group of the Witwatersrand basin exhibits extensive lateral variation.

doi:10.2113/gssajg.113.1-1

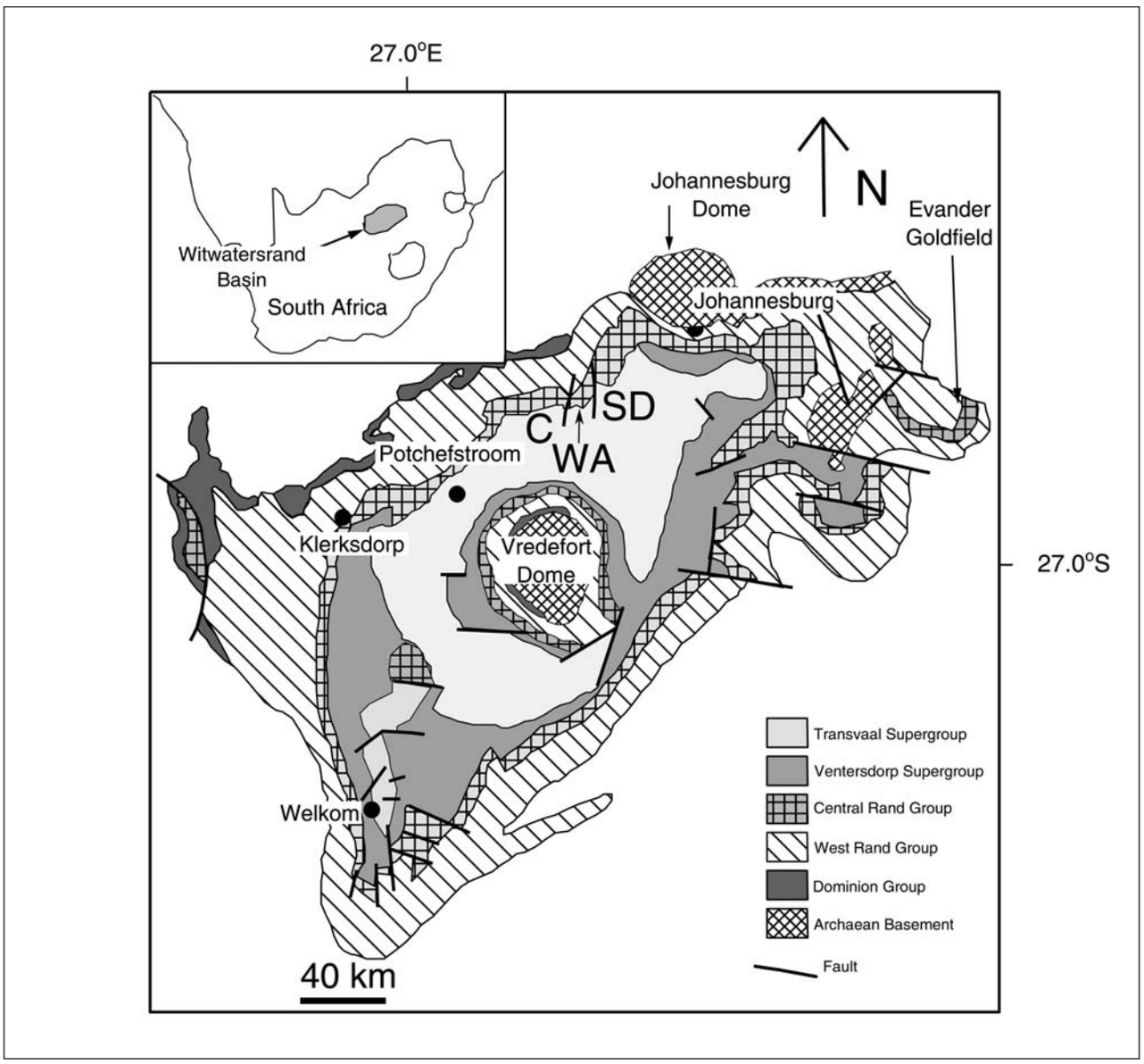

Figure 1. A simplified geological map of the Witwatersrand Basin showing the distribution of the main geological groups, as well as the position of the studied samples. C = Carltonville, WA = Western Areas, SD = South Deep. (from Frimmel and Minter, 2002). TauTona mine is in the Carltonville area.

The vertical variation in gold mineralization within the Carbon Leader Reef package also varies on a centimetre scale. Mine geologists currently rely on sedimentary facies models to evaluate ore reserves and the effect (if any) of hydrothermal metamorphic activity might lead to ore resource models that are less accurate and not always reliable.

The aims of this paper are as follows:

1. To determine the hydrogen and oxygen isotope composition of the Carbon Leader Reef at TauTona and Savuka mines, and identify any lateral and vertical variation;
2. To determine the isotope and chemical composition of the fluid(s) that interacted with the Carbon Leader Reef at TauTona mine;
3. To characterize the nature of fluid-rock interaction and identify any relationship between the fluid-rock interaction and gold mineralization.

Location and background of the study

Most samples were obtained from TauTona Mine, an AngloGold Ashanti gold mining operation that is situated in the Carltonville Goldfields within the Witwatersrand Basin (Figure 1). A smaller number of samples were obtained from the nearby Savuka Mine, 6 km west of TauTona. The area is located approximately 80 km southwest of Johannesburg (Figure 1). TauTona Mine has been operating since 1962 and was originally known as Western Deep Levels 3 shaft. Savuka was previously known as Western Deep Levels 2 shaft.

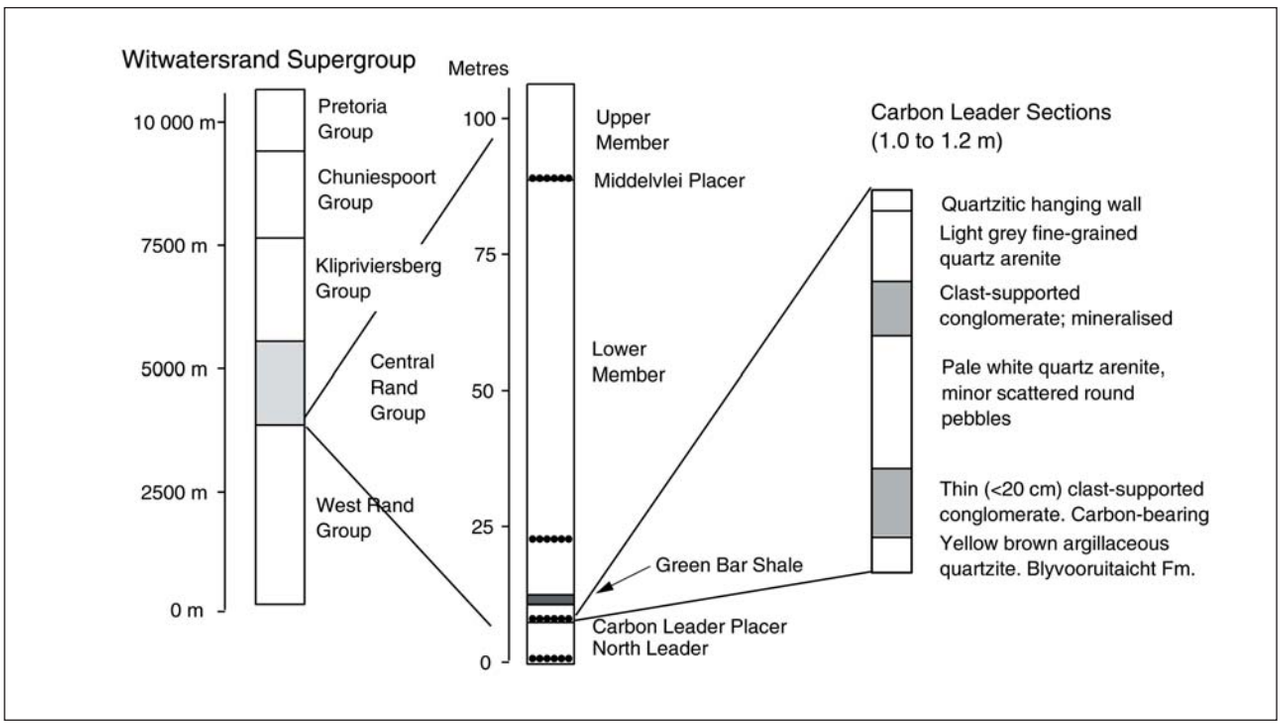

Figure 2. A simplified representation of the stratigraphic column of the Witwatersrand Supergroup, showing the position of the Carbon Leader just above the boundary between the West and Central Rand Groups. Also shown is the lithostratigraphic subdivision of the lower ~100 m of the Johannesburg Subgroup showing the stratigraphic position of the Carbon Leader (from Karpeta and Els, 1999), and a schematic section through the Carbon Leader in the study area.

Both mines are among the deepest gold mines in the world, with a maximum depth of 3476 m below surface. The Carbon Leader Reef is economically the most important unit within the gold bearing conglomerates of the Central Rand Group. At the time of writing, the Carbon Leader Reef is the main reef mined at TauTona Mine and is responsible for 95% of the gold produced. The Ventersdorp Contact Reef (VCR), which is located about 700 m stratigraphically above the Carbon Leader Reef, currently accounts for the remaining 5% of gold production (Mineral Resources Statement, 2006).

Geological setting

The West Wits Line (Engelbrecht et al., 1986), also known as the Carltonville Goldfields, consists of numerous economically viable conglomerate horizons, and is situated on the north-western edge of the Witwatersrand basin (Figure 1). The Witwatersrand Supergroup comprises the West Rand Group having a maximum thickness of 5.15 km, which is overlain unconformably by the Central Rand Group having a maximum thickness of 2.88 km (e.g. Frimmel 2006). The metasedimentary rocks of the West Rand Group are believed to have been deposited in distal fluvio-deltaic and shoreface to offshore environments, which fluctuated due to eustatic sea level changes (Stanistreet and McCarthy, 1991). The sandstone to shale ratio is about 1:1 in the West Rand Group, whereas it is much higher in the overlying Central Rand Group (Frimmel, 2006). The Carbon Leader Reef is a relatively thin (up to 1.2 m) but persistent unit that unconformably overlies the Blyvooruitzicht Formation, which is the lowest Formation in the Central Rand Group (Figure 2). The conglomerates of the Central Rand Group were deposited in a series of fluvio-deltaic processes and shallow marine systems, and extensive tidal reworking due to transgression and regression of sea level is common (Karpeta and Els, 1991). The sediment deposition of the Central Rand Group is thought to be controlled by fault related uplift to the east and palaeocurrent orientations show potential provenance of sediments to the north and north-east (Frimmel et al. 2005).

The sedimentary rocks of the Witwatersrand Supergroup were covered by lavas of the Ventersdorp Supergroup and this magmatic activity was followed by the continuous deposition of sedimentary rocks of the Transvaal Supergroup. At ~2.06 Ga (Buick et al., 2001), intrusion of the Bushveld Igneous Complex and its associated satellite bodies caused a steep rise in the geothermal gradient (Frimmel, 1994). This, in addition to the catastrophic event associated with the Vredefort meteorite impact at ~2.02 Ga (Moser, 1997), means that the Witwatersrand Basin was affected by both burial metamorphism as well as additional thermal perturbations, and this may have enhanced fluid flow (e.g. Robb et al. 1995). Geothermobarometry on

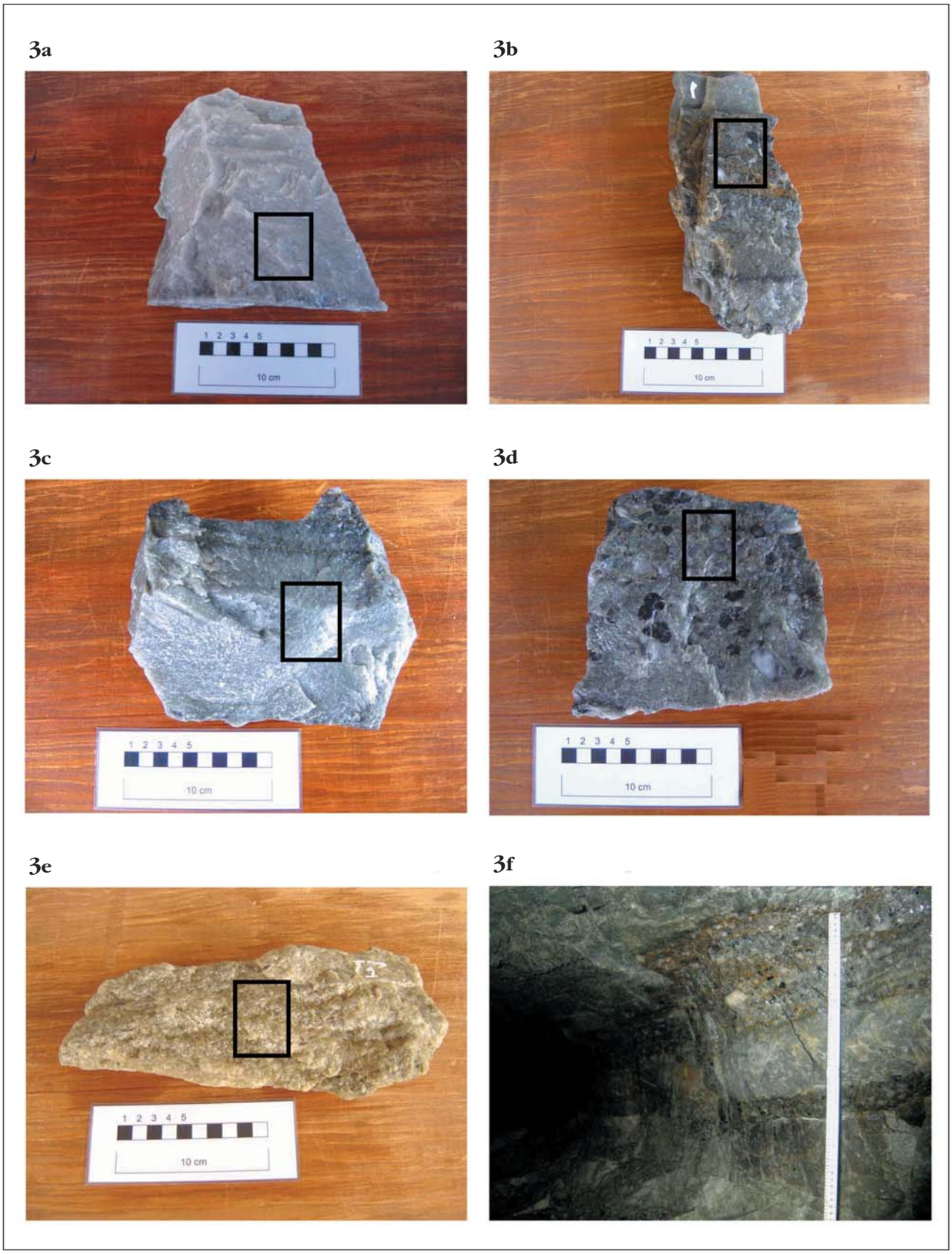

Figure 3. Photographs of samples taken from the Carbon Leader reef at Tau Tona Mine, showing the major rock types. (**a**) the hangingwall quartzite, (**b**) upper conglomerate, (**c**) middle quartzite, (**d**) lower conglomerate and (**e**) the footwall quartzite (Blyvooruitzicht Formation). The black squares indicate the portion of each sample used for isotope analysis. (**f**) The Carbon Leader Reef at Tau Tona Mine looking down dip towards the south, showing the nature and thickness of the different units. Clino-rule = 1 m.

hydrothermal chlorite yielded peak metamorphic conditions in the greenschist facies of 300°C to 350°C, at pressures ranging from 2.5 to 3.0 kbar (Frimmel, 1994; Robb and Meyer, 1995). Frimmel and Minter (2002) suggested that these regional peak metamorphic conditions were achieved during deposition of the Pretoria Group.

The Carbon Leader Reef in the study area is stratigraphically overlain by quartzites of the Main Formation. The Carbon Leader Reef package studied comprises an 80 to 100 cm thick tabular, auriferous unit (Figure 2). The lower part consists of a basal conglomerate that grades upwards into sandstone, which in turn is overlain by a second conglomerate, which also grades upwards into sandstone (Figure 3). The conglomerates are typically quartz-pebble supported and are seldom more than 20 cm thick. The thickness of the sandstone units is highly variable, and this appears to be due to sedimentary processes. Distinct cross bedding features can be seen in the sandstone units, which are emphasized by concentration of pyrite grains along the foresets. At the base of the basal conglomerate is a thin (less than 10 mm) carbonaceous seam. In the study area, the Carbon Leader package dips at 22° to the south. The distribution of Au in the studied samples is unknown, but Engelbrecht et al. (1986) point out that Au in the Carbon Leader Reef occurs variably as veinlets, specks, and anhedral grains, and is mainly associated with sheet silicates infilling cracks and cavities in the carbonaceous material. Mossman (2008) discussed the origin of carbonaceous material in Witwatersrand rocks and concluded that both kerogen (remains of former living organisms) and bitumen (macromolecular organic compound which was once mobile as a viscous fluid but which has since solidified) are present. The distinction between the two was not made in this study and such material will be referred to as carbonaceous material.

Previous O- And H-isotope Studies of the Wits

Harris and Watkins (1990) determined the $\delta^{18}O$ value of various whole-rock samples of the Witwatersrand Supergoup and found a range from 8.6 to 10.3‰ (mean 9.7‰). Barton et al. (1992) and Vennemann et al. (1992) reported oxygen isotope data on quartz pebbles from the Witwatersrand Supergroup in an attempt to identify their provenance. Both studies revealed significant variation in the $\delta^{18}O$ values of different quartz pebbles within individual samples, and these authors concluded that the pebbles had not changed their $\delta^{18}O$ values since deposition. On the basis of a comparison of quartz pebble $\delta^{18}O$ values with those of potential Archaean source material, Vennemann et al. (1992) suggested that the source was a mixture of vein quartz, and quartz derived from granite pegmatites. A subsequent more detailed study by Vennemann et al. (1995) on the Monarch and Main Reefs showed that that the $\delta^{18}O$ of quartz pebbles range from 8.8‰ to 14.5‰. The $\delta^{18}O$ value of sand-sized quartz grains within the matrix of the Monarch and Main Reefs ranged from 7.8‰ and 11.8‰. This is lower than the range for quartz pebbles, and Vennemann et al. (1995) suggested that this is due to a difference in provenance. Zhao et al. (2006) determined the $\delta^{18}O$ and δD values for separated muscovite from the Ventersdorp Contact Reef and used them to estimate the composition of the fluid ($\delta^{18}O$ 4.8 to 6.1 ‰; δD -27 to –39 ‰), which they suggested was metamorphic in origin. Fagareng et al. (2008) determined the $\delta^{18}O$ and δD values of a number of Witwatersrand Supergroup samples in the collar of the Vrederfort Dome. Metapelites in the Vredefort collar have a $\delta^{18}O$ value averaging 7.7‰ (n = 45), and whole-rock δD values averaging -62‰. Fagareng et al (2008) pointed out that the collar rocks had unusually low $\delta^{18}O$ values for siliciclastic sedimentary rocks and suggested that impact-induced secondary permeability enhanced interaction with fluids.

Methodology

Sample collection

Four sample sections through the Carbon Leader Reef were chosen, with a range of Au contents. At each sample location, four to six samples were taken to give a complete cross section of the Carbon Leader Reef. The samples consisted either of medium-grained quartzite with intermittent pebble lags, or small pebble conglomerates (Figure 4). Three sample traverses were taken at TauTona Mine over a total distance of about 200 m down dip. A sample traverse was also made through the Carbon Leader Reef at the adjacent Savuka Mine, situated approximately 6 km west of Tau Tona.

Analytical techniques

The volume % of matrix, detrital quartz pebbles and grains, authigenic quartz, chloritoid, white mica and opaque minerals present in each were determined by point counting. A total of 3000 counts were made on a single thin section of each sample in order to obtain a reasonable statistical representation.

All oxygen and hydrogen isotope data were obtained at the University of Cape Town. The isotope ratios were measured using a gas-source Finnegan Mat DeltaXP mass spectrometer in dual inlet mode, and the results are reported in standard δ-notation relative to SMOW. For oxygen isotopes, 10 mg of whole-rock powder were analysed using conventional Ni reaction vessels. Ten samples were loaded in each sample run, of which two were the NBS28 quartz standard. Oxygen was produced by reaction with ClF_3 at 550°C for at least four hours. The average value obtained for the NBS28 samples was used to normalize the raw data in each run to the SMOW scale assuming a value of NBS28 of 9.64‰. In practise, the difference between the raw and normalised data was < ~0.5‰. During the analysis of oxygen isotopes in this study the average difference between duplicate NBS28 analyses was ± 0.16‰ this is an equivalent of 1σ of 0.21‰. For hydrogen, the method of Vennemann and O'Neil (1993) was used.

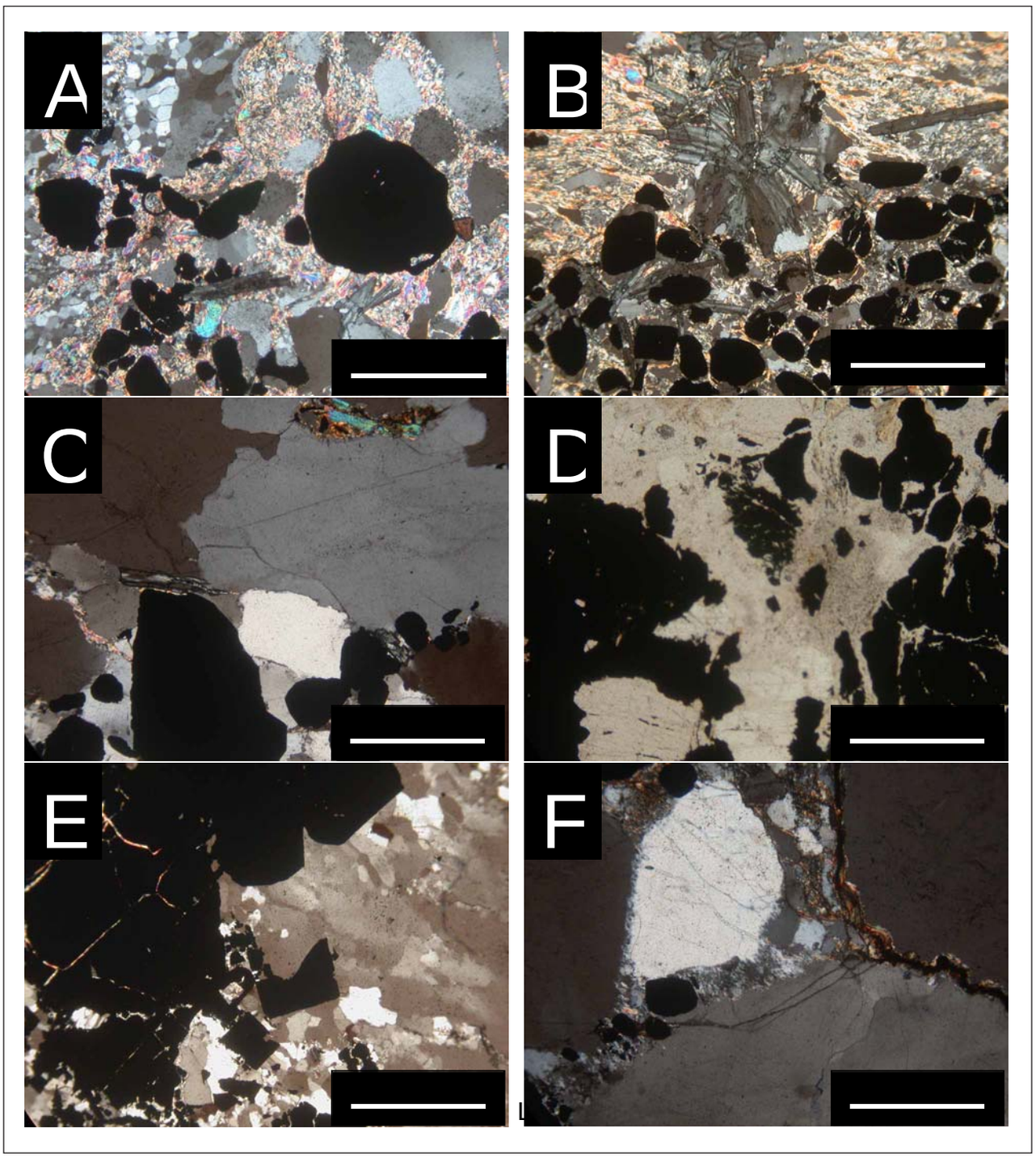

Figure 4. Photomicrographs of the Carbon Leader Reef. (**a**) Anhedral opaque minerals within a matrix supported quartzite with angular detrital quartz grains. Note the authigenic quartz crystals in the top left hand corner. (**b**) Chloritoid crystals with needle like morphology within the matrix of white mica. The opaque minerals are associated with the chloritoid. (**c**) Large opaque minerals crystallized over some quartz. Note the opaque minerals are not restricted to the matrix in this sample. (**d**) Organic matter (opaque mineral) present between the quartz grains (ppl). (**e**) Cubic nature of the pyrite in the centre is clearly distinguishable from the organic matter on the left hand side. (**f**) The dissolution of the quartz grain boundary is very clear, the matrix crystallized in expense of detrital quartz.

Approximately 100 mg of each sample was placed into quartz-glass tubes that had been roasted at 800°C and stored at 110°C before use. The samples were dried overnight at 110°C before the extraction of water by pyrolysis at ~1200°C. The water released was collected in "break seal" tubes filled with 10 mg of "Indiana Zinc" to reduce the water to H_2. Two internal standards of Cape Granite biotite (CGBi; δD = -57‰) were analysed during each run of ten samples. The average reproducibility of this standard during the study was

Table 1. Oxygen and hydrogen isotope data, water content and mineral concentration for bulk rock samples of the Carbon Leader Reef

Sample	Lithology	δD	Water wt.%	$\delta^{18}O$	Mineral Concentration (%)						Au (ppm)
					Detrital quartz	Authigenic quartz	Chloritoid	Matrix	Opaque material	Hydrous minerals	
A1-1	FQ	-27	1.04	10.7	63.8	6.4	4.5	25.3	0.1	29.8	0.0
B1-1	FQ	-45	0.74	9.7	66.1	10.4	2.8	20.5	0.2	23.3	3.8
B2-1	FQ	-27	3.31	7.2	55.7	3.4	1.1	12.9	26.8	14.0	5.0
A2-1	BC	-26	0.65	10.4	62.1	18.3	1.4	14.5	3.0	15.9	9.5
B1-2	BC	-45	0.96	9.9	59.5	4.1	4.3	31.3	0.8	35.5	5.3
C1-1	BC	-52	0.67	10.2	60.3	20.1	0.0	19.3	0.4	19.3	104.0
D2-3	BC	-63	0.37	10.5	75.3	8.0	1.5	14.5	0.8	16.0	15.4
A3-3	MQ	-37	0.67	10.8	68.5	15.9	3.6	12.0	0.0	15.6	0.3
C2-2	MQ	-59	0.34	10.8	61.1	5.4	3.3	6.4	22.5	9.7	5.9
C3-1	MQ	-34	0.87	10.2	68.3	7.3	1.4	22.2	0.9	23.6	174
D2-2	MQ	-65	0.36	10.3	76.6	13.4	0.1	9.3	0.5	9.5	7.8
B2-2	MQ	-58	0.40	9.6	82.7	5.9	1.2	9.9	0.3	11.1	4.9
B2-3	MQ	-45	0.41	9.9	70.7	14.3	1.3	13.8	0.1	15.1	5.5
X1-1	MQ	-35	0.58	10.3	70.7	13.2	3.5	12.0	0.6	15.4	3.2
A5-1	UC	-36	0.87	10.5	55.8	7.2	3.1	33.8	0.1	36.9	33.9
B3-1	UC	-49	0.52	10.5	69.4	2.8	4.0	19.5	4.2	23.5	5.4
C3-2	UC	-27	0.83	10.5	67.5	6.2	1.1	24.5	0.7	25.6	174
C3-3	UC	-36	0.73	10.0	71.3	7.4	1.6	17.6	2.1	19.2	174
D3-1	UC		2.29	9.8	55.3	1.0	2.6	10.0	31.0	12.6	42.7
A5-2	HC	-32	0.85	10.4	66.0	10.7	1.7	21.3	0.3	23.0	33.9
B4-2	HC	-59	0.66	10.4	73.8	4.1	8.3	13.7	0.1	22.0	6.7
C3-4	HC	-29	0.71	10.6	64.4	7.2	1.5	26.3	0.6	27.8	174
D4-1	HC	-43	0.49	10.8	72.3	13.5	0.0	14.2	0.1	14.2	0.0

Note: FQ-Footwall Quartzite, BC-Bottom Conglomerate, MQ-Middle Quartzite, UC-Upper Conglomerate, HQ-Hangingwall Quartzite. The Au concentration is not sample-specific. But the average for the unit in the immediate vicinity of the sample site. Hence all C3-X samples have the same Au concentration. X1-1 is a quartzite collected from the vicinity of A1-1

± 3.1‰. An internal water standard (CTMP; δD = -9‰) was used to normalise the data to the SMOW scale. The weight percentage of water for each sample was determined during the introduction of the H_2 to the mass spectrometer with the inlet section set to a fixed volume. The relative error for water content is ± 1.25% for a sample yielding 2 mg of water (Fagereng et al., 2007).

The gold concentration of the samples was provided by the evaluation department of AngloGold Ashanti. The gold concentrations of the samples were determined on 50 g of samples using the lead fusion method, by SGS Geochem Services. The precision is 5% at the 1 g/ton level.

Petrography of studied samples

The conglomerate horizons consist of small (7 to 24 mm) clear, milky and smoky quartz pebbles (Figure 4). The general mineralogy of the conglomerates is that of very fine-grained anhedral detrital quartz crystals, authigenic quartz, muscovite, chlorite, chloritoid, pyrophyllite, carbonaceous material and opaque minerals. Some detrital zircon grains and traces of rutile are also present in several samples. Table 1 gives the modal proportions of the most abundant minerals present in the samples.

Quartz is the major constituent of all of the samples and is present in the form of detrital and authigenic quartz grains. Detrital quartz accounts for 50 to 80% of all material present (Table 1) whereas the authigenic quartz comprises up to 20% (average ± 9%). Smaller detrital quartz grains show relatively irregular shapes, and several quartz crystals show corroded boundaries where it is in contact with the matrix (Figure 4e). Sutured quartz grain boundaries occur between adjacent quartz grains and chlorite and white mica may be present on the grain boundaries. Diagenetic quartz overgrowths may also be present. Authigenic quartz may also appear as isolated clusters within the general matrix and have granoblastic texture (Figure 4a).

Up to 5% of the bulk rock consists of chloritoid crystals that are generally euhedral and typically range from 100 to 500 μm, although chloritoid crystals of 1.5 mm are present in certain samples. The chloritoid crystals typically show acicular texture and, in general, are in direct contact with detrital quartz. However, some chloritoid crystals are found within the matrix (Figure 4b) and Barnicoat et al. (1997) interpreted this to indicate that chloritoid crystallization post-dated the matrix mica void-fill, and that chloritoid formed only after burial metamorphism. The matrix consists predominantly of white mica, with small quantities of

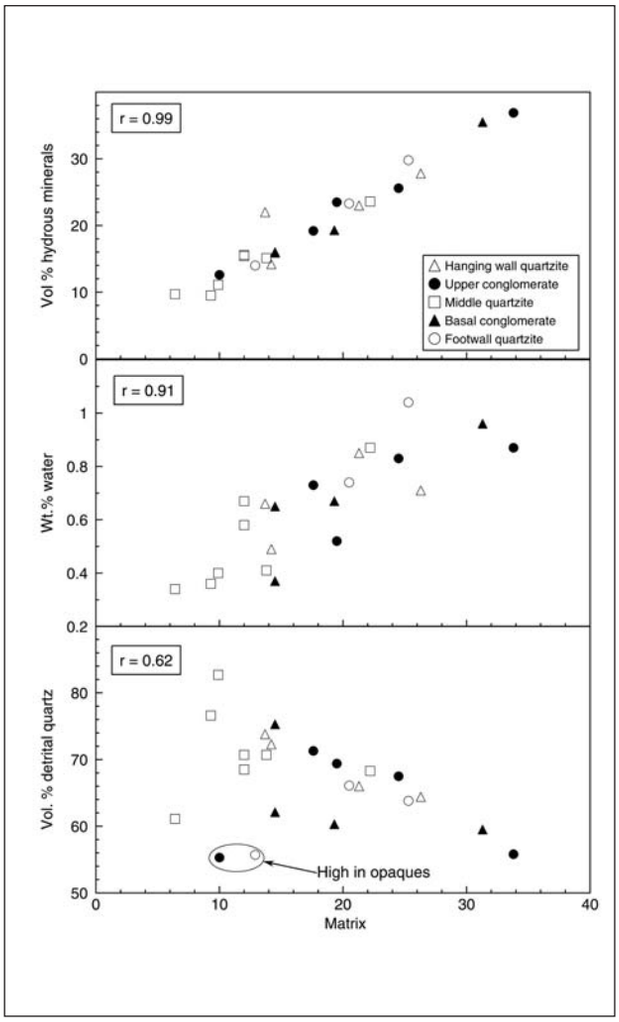

Figure 5. Plot of volume % hydrous minerals, wt.% water and volume % detrital quartz vs. volume % matrix for the studied samples. All data determined by point counting (see text).

pyrophyllite and chlorite, and accounts for between 6% and 34% of the bulk rock. It generally fills the interstitial spaces between the detrital quartz grains.

The opaque material present appears to be either pyrite or carbonaceous material, and these show different characteristics in shape and size, as well as the distribution. They account for about 5% of the bulk rock although several samples had as much as 22% opaque material. Authigenic pyrite is very distinct and easily recognisable by the cubic crystal shape (Figure 4e). The authigenic pyrite crystals range in size from 100 to 300 μm and have clearly overgrown some of the detrital quartz crystals and matrix minerals. The authigenic pyrite crystals also appear to be in close association with chloritoid relative to the spatial distribution and some chloritoid crystals enclosed pyrite crystals in certain instances, suggesting a relative chronology of mineral crystallisation (Figure 4b). Barnicoat et al. (1995) suggested that the paragenetic stages for the Carbon Leader are firstly diagenetic quartz overgrowth with minor white mica and chlorite, chloritoid and pyrophyllite followed by pyrite and uraninite. Small quantities of smaller, more rounded opaque minerals that are associated with detrital zircons are present and sparsely distributed and are interpreted as detrital pyrite grains. In several of the samples taken from the basal conglomerate, large irregular masses of opaque material are present (Figure 4d). This opaque material has overgrown and overprinted most of the minerals present and is interpreted to be of late stage introduction of hydrocarbon (Frimmel et al. 2002).

Although the results presented in this paper offer no insights into the origin of the carbonaceous matter, we concur with Mossman et al (2008) that the carbon is of biogenic origin. A detailed carbon isotope study by Spangenberg and Frimmel, (2001) gave a mean $\delta^{13}C$ value of -26.0‰ in the Witwatersrand carbon-bearing seams as a whole and these authors concluded that biogenic organic matter buried in sediments was the source of the hydrocarbons.

Selected modal data are presented graphically in Figure 5. The modal % hydrous minerals shows a very strong correlation with % matrix (r = 0.99), which is consistent with the matrix being dominated by hydrous minerals. The amount of water (determined during H-isotope analysis) also shows a good correlation with modal % matrix (r = 0.91). The middle quartzite has generally less matrix and less water than the other rock types, otherwise there is little relationship between rock type and volume % matrix. There is a negative correlation between the volume % detrital quartz and

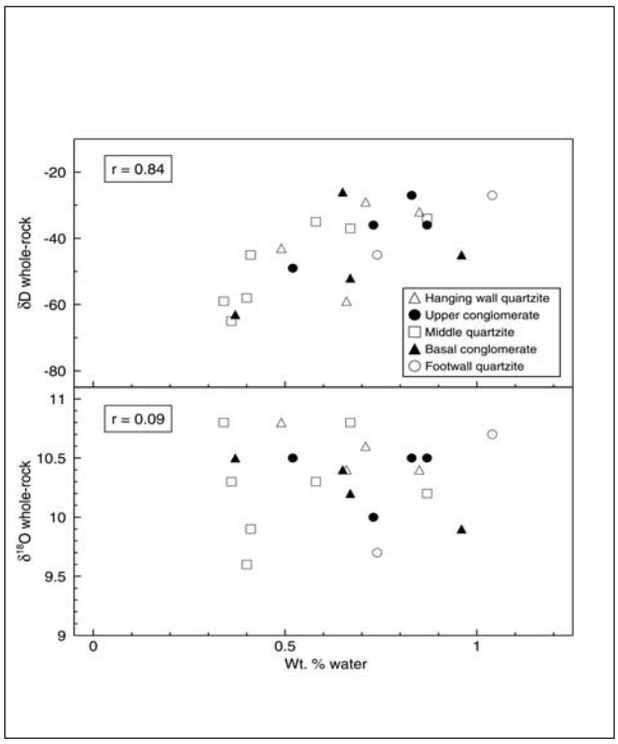

Figure 6. Plot of bulk-rock δ18O and δD values vs. wt. % water in Carbon Leader samples.

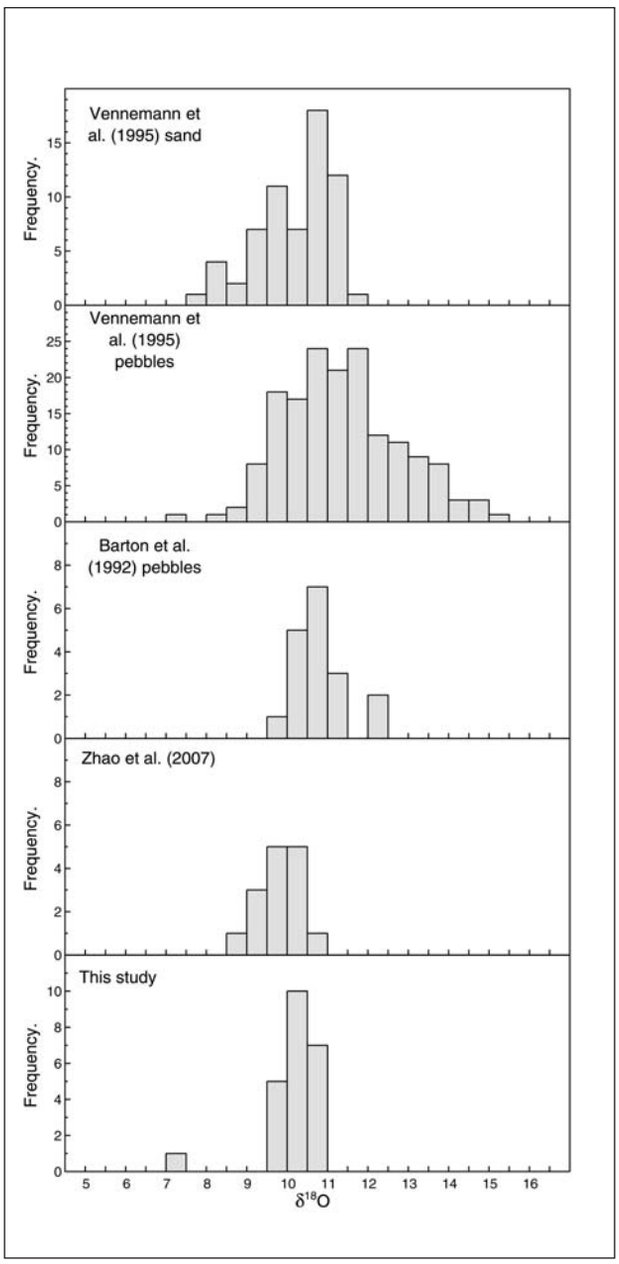

Figure 7. Histogram of the δ18O values for the bulk rock samples showing the range of δ18O values. The class interval was 0.5‰, e.g. 10.00‰ to 10.49‰, inclusive. Also shown are histograms for quartz pebbles and sand grains from gold-bearing rocks from the Witwatersrand Basin (Vennemann et al. 1995), quartz pebbles from the Witwatersrand Basin analysed by Barton et al. (1992), and bulk-rock samples from the vicinity of the Ventersdorp Contact Reef (Zhao et al. 2006)

volume % matrix (r = -0.62). The main reason why the correlation is not stronger is probably the presence of detrital opaque material. The volume % of chloritoid shows no significant correlation with either the % matrix (r = 0.34) or the % water (r = 0.62).

Results

The $\delta^{18}O$ and δD values and water content of the bulk rock samples are given in Table 1, and presented visually in Figures 6 to 8. The range of $\delta^{18}O$ values is relatively restricted, between 9.6‰ and 10.8‰, with a mean value of 10.12‰ ± 0.74‰ (1σ, n = 22). The one exception is sample B2-1 with $\delta^{18}O$ value of 7.2‰, which has been excluded from the calculated mean value and is not plotted on Figure 6. Sample B2-1 is one of three samples with a high content of opaque material, and the $\delta^{18}O$ value should be treated with caution as the presence of significant amounts of sulphide and/or carbonaceous material might have affected the extraction of O from this sample during analysis. Given the small range in $\delta^{18}O$ values, it is not surprising that there are no systematic stratigraphic or lateral variations in bulk rock $\delta^{18}O$ values. There is no correlation between bulk rock $\delta^{18}O$ value and the wt. % water (Figure 6) or any mineralogical parameter (modal % matrix, chloritoid etc).

The δD values of 22 samples from the Carbon Leader Reef range from -63‰ to -26‰, with an average of -42‰ ± 12‰ (1σ, n = 22). The bulk rock δD value shows a positive correlation with wt. % water (r = 0.84). Although the range of δD values is relatively large, there are no systematic differences between the various lithological units of the Carbon Leader. The water content of the bulk samples range from 0.34 wt. % to 1.04 wt. % with a mean of 0.65 wt % ± 0.20 wt. % (1σ, n = 21) with the exception of samples B2-1 and D3-1 with water content of 3.31 wt. % and 2.29 wt. %, respectively, which are treated as outliers and excluded from the calculated mean value. The high water content in these samples is presumably due to the presence of carbonaceous material (both samples have >20% (opaque material). Any H in the carbonaceous material would be converted to water as a result of the extraction procedure and the δD values obtained for these two samples must largely reflect those of the carbonaceous material. That the values obtained (-27 and -59‰) are not highly negative is surprising given that this is H associated with reduced carbon. Further discussion is beyond the scope of this paper, but further investigation is warranted.

Discussion

Our data are compared to previously published data on the Wits in Figure 7. Our $\delta^{18}O$ values are extremely similar to the results of Barton et al. (1992) for samples from throughout the Witwatersrand Supergroup and Zhao et al. (2006) for the Venterdorp Contact Reef. Vennemann et al. (1995) reported the $\delta^{18}O$ values of both pebbles and sand sized grains from a large number of different gold reef. These authors found a somewhat larger spread of data for both sand grains and pebbles with the sand grains having, on average, slightly lower $\delta^{18}O$ values. Nevertheless, the mode for our data (Figure 7) corresponds very closely to mode for the Vennemann et al. (1995) data.

Unlike Vennemann et al. (1992; 1995) and Barton et al. (1992), we did not analyse individual quartz

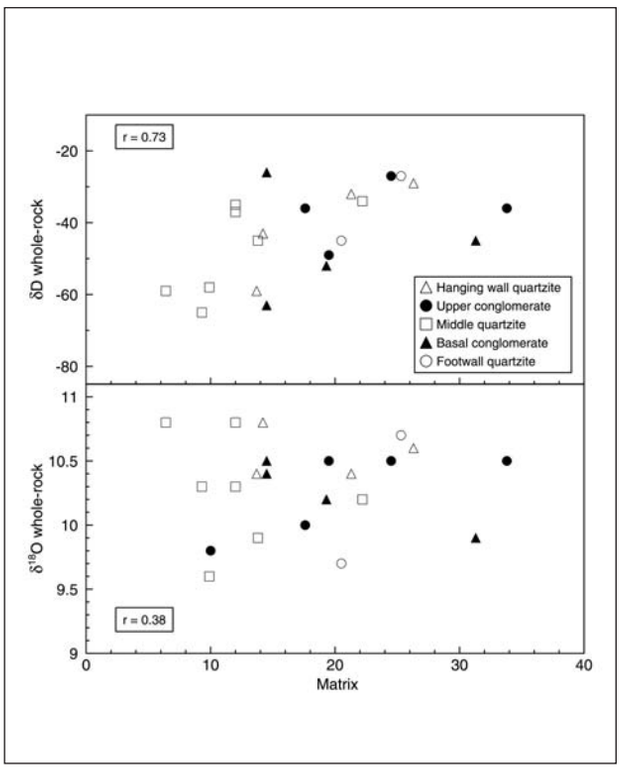

Figure 8. Plot of bulk rock δ18O and δD values vs. volume % matrix.

pebbles, or separated matrix material. However, it is possible to estimate the isotope composition of matrix material with reference to a plot of bulk rock $\delta^{18}O$ value vs. the amount of matrix (Figure 8). The lack of significant correlation (r = 0.38) indicates that the $\delta^{18}O$ value of the matrix is not significantly different to that of the detrital quartz in the Carbon Leader Reef. However, there is a more significant correlation (r = 0.73) between whole-rock δD values and the amount of matrix. This suggests that the detrital minerals have more negative δD values than the matrix material.

The isotope composition of the fluid in equilibrium with Carbon Leader Reef can be estimated using a range of fractionation factors. In this study, only bulk rock samples were analysed, and the assumption is made that the fractionation factor for each rock is a product of the sum of the fractionations of the individual minerals and their respective mole fraction (e.g. Vry et al. 2001; Fagereng et al. 2007) The mole fractionations have been estimated from the volume % determined by point-counting (Table 1). A temperature of 350°C was assumed to be the temperature of the fluid-rock interaction based on the metamorphic minerals present (see above and Frimmel, 1994). The estimated bulk rock-water fractionations are given in Table 3 as are the mineral-water fractionation factors used. As discussed above, this temperature corresponds to that of peak metamorphism. If a temperature of 300°C is used, $\Delta_{rock\text{-}water}$ calculated from the equations in Table 3 would be about 1.5‰ higher. This means that the fluid $\delta^{18}O$ values (Figure 9) would shift to values that are 1.5‰ lower.

For hydrogen, it was assumed that the δD values of the bulk sample can be approximated by that of the hydrous minerals in the matrix. It was further assumed that the fluid equilibrated with only white mica. The other hydrous minerals are chlorite and chloritoid. The fractionation factor for chlorite ($\Delta_{chlorite\text{-}water}$ = -35‰, Taylor, 1974) is similar to that of muscovite at 350°C, and there are no published fractionation factors for chloritoid. In any case the abundance of white mica greatly exceeds that of the other hydrous minerals. Published fractionation factors for muscovite (Suzuoki and Epstein, 1976) and illite (= white mica) (Sheppard and Gilg, 1996) are slightly different, and fluid δD values were calculated using both (Table 2, Figure 9). The effect on δD of a lower temperature of metamorphism is uncertain because of the general uncertainty of H-isotope fractionation factors

The bulk-rock and calculated fluid compositions are represented on a δD vs $\delta^{18}O$ plot (Figure 9) from which it is evident that the majority of the samples were in equilibrium with fluids that have compositions expected for metamorphic water (Figure 9). There is no correlation between δD and $\delta^{18}O$ (Figure 9) and there is no significant difference in isotope composition between different rock types. Magmatic water could have been a possible source of the hydrothermal fluid but can be discounted because the estimated fluid δD values are

Table 2. Fractionation factors and calculated O- and H-isotope composition of fluid in equilibrium with bulk rock

Sample	δD WR	δD W	$\delta^{18}O$ WR	$\delta^{18}O$ W	Δr-w H	Δr-w O
A1-1	-27	-2	10.7	5.4	-25	4.3
A2-1	-26	-1	10.4	5.1	-25	4.6
A3-3	-37	-12	10.8	5.5	-25	4.8
A5-1	-36	-11	10.5	5.2	-25	4.2
A5-2	-32	-7	10.4	5.1	-25	4.6
B1-1	-45	-20	9.7	4.4	-25	4.6
B1-2	-45	-20	9.9	4.6	-25	4.1
B2-1	-27	-2	7.2	1.9	-25	3.5
B2-2	-58	-33	9.6	4.3	-25	4.9
B2-3	-45	-20	9.9	4.6	-25	4.8
B3-1	-49	-24	10.5	5.2	-25	4.3
B4-2	-59	-34	10.4	5.1	-25	4.5
C1-1	-52	-27	10.2	4.9	-25	4.7
C2-2	-59	-34	10.8	5.5	-25	3.7
C3-1	-34	-9	10.2	4.9	-25	4.5
C3-2	-27	-2	10.5	5.2	-25	4.5
C3-3	-36	-11	10.0	4.7	-25	4.6
C3-4	-29	-4	10.6	5.3	-25	4.4
D2-2	-65	-40	10.3	4.9	-25	5.0
D2-3	-63	-38	10.5	5.2	-25	4.8
D4-1	-43	-18	10.8	5.5	-25	4.9
X1-1	-35	-10	10.4	5.1	-25	4.7

Fluid composition calculated for 350°C. WR = whole-rock, W = water, Dr-w = per mil fractionation between rock and water.

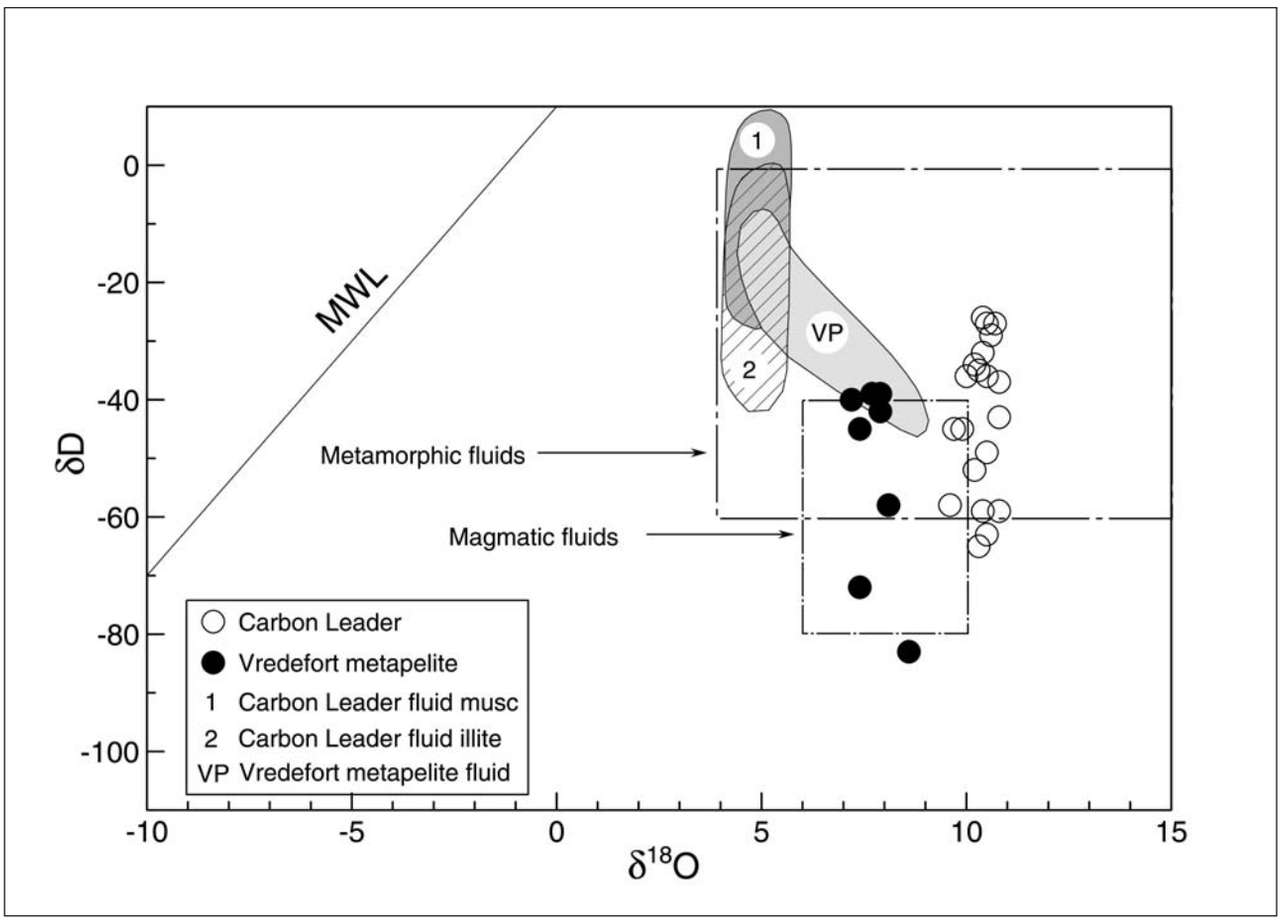

Figure 9. A plot of δD versus δ18O of the bulk-rock samples of Carbon Leader Reef. The fields for metamorphic- and magmatic water (Sheppard, 1986), and the global meteoric water line (Craig 1961) are also shown. Composition of fluids calculated using the muscovite-water fractionation equation (Field 1) of Suzuoki and Epstein (1976), and illite-water (Field 2) of Sheppard and Gilg (1996), assuming a temperature of 350°C. Witwatersrand Supergroup metapelite data from Fagareng et al. (2008) and fluids in equilibrium with them at peak metamorphic temperatures (450 to 500°C) also plotted.

too high (Figure 9). A major magmatic event, such as the intrusion of the Bushveld Igneous Complex, could, have provided the heat to drive the infiltration and circulation of surface water. This was considered unlikely by (Frimmel et al., 2005) because the primary permeability of the Witwatersrand sediments would have been substantially decreased due to burial processes and dehydration caused by low-grade metamorphism that predates the Bushveld event. Fagereng et al. (2008) identified low $\delta^{18}O$ values in Vredefort collar metapelites that represent the more distal part of the Witwatersrand basin and explained these data as being due to relatively high degrees of fluid-rock interaction. The samples analysed in the present study do not have unusually low $\delta^{18}O$ values for clastic sedimentary rocks.

Frimmel et al. (1999) proposed that extensive fluid flow in the Witwatersrand basin rocks was aided by the creation of impact-induced secondary permeability at the time of the Vredefort impact. The dense network of micro-fractures developed in the already metamorphosed Witwatersrand rock sequence enabled the interaction between rock and fluid. These authors further argued that after progressive burial metamorphism reached lower greenschist facies conditions in the lower part of the Witwatersrand Basin, the primary permeability and any connate water would have disappeared. They pointed out that a tectonic event, like the Vredefort impact, would have been required to increase the secondary permeability, and that the up-turning and fracturing of the rocks around

Table 3. MISSING CAPTION

Fractionation factors used		
Phases	**1000 ln α***	**Reference**
Oxygen isotope fractionation factors		
quartz-H_2O	3.38 ($10^6/T^2$) – 3.4	Matsuhisa et al. (1979)
muscovite-H_2O	2.38 ($10^6/T^2$) – 3.89	O'Neil and Taylor (1969)
Hydrogen isotope fractionation factors		
muscovite-H_2O	-22.1 ($10^6/T^2$) + 19.1	Suzuoki and Epstein (1976)
Illite-H_2O	-25	Sheppard and Gilg (1992)
chlorite-H_2O	-45 to -35**	Taylor (1974)

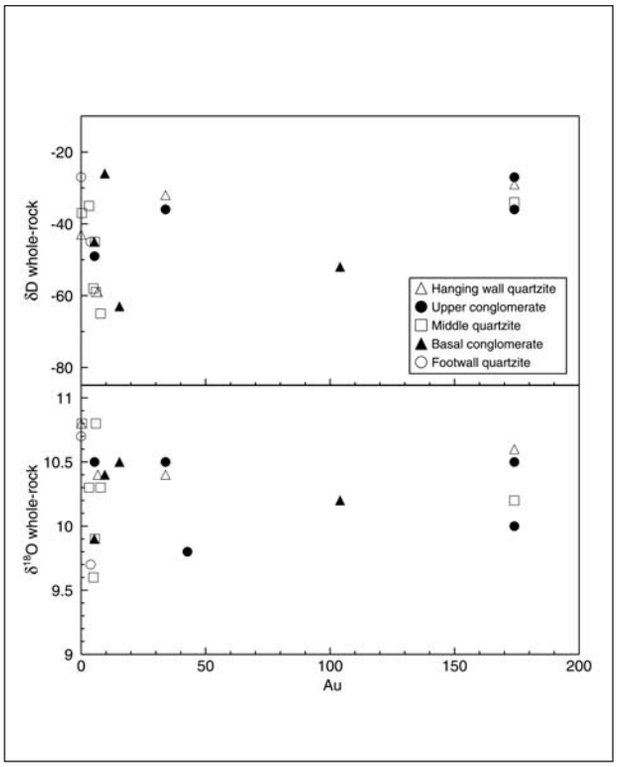

Figure 10. Plot of bulk rock δ18O and δD values vs. Au content. Note that the Au content is for samples from the immediate vicinity and does not correspond exactly to the sample analysed.

the impact site, together with a significant disturbance of the geotherm would have permitted surface waters to reach depths as great as 10 to 15 km.

The nature of the fluids present during metamorphism of the Witwatersrand Basin rocks was discussed by Drennan et al. (1999) who, on the basis of fluid inclusion studies concluded that that the earliest recognisable inclusion fluids were H_2O and H_2O-CO_2 dominated, with later fluids being lower temperature, hydrocarbon-bearing, low-density fluids (giving rise to vapour-rich inclusions). Klemd (1999) investigated hydrothermal alteration of the basement granitoids surrounding the Witwatersrand Basin and identified high-salinity $CaCl_2$-rich fluids as being derived by the dewatering of the Witwatersrand basin. Frimmel et al (1999) concluded that two gold-mobilizing events affected the Witwatersrand Basin, one at early Transvaal times, the other at the time of the Vredefort impact. On the basis of fluid $\delta^{18}O$ values close to 0‰ estimated from O-isotope data on quartz veins, Frimmel et al. (1999) suggested a substantial meteoric component in those fluids, and Frimmel (2008) suggested that the initial fluid–rock interaction most probably involved leaching by basin-wide penetration of meteoric water shortly after sediment deposition. He suggested several stages of enhanced fluid circulation through the Witwatersrand Basin ranging from diagenetic basin dewatering to later hydrothermal fluid infiltration events.

The data presented in this paper are consistent with Wits Basin fluids being metamorphic in origin, but the composition of basin brines worldwide is sufficiently variable (e.g. Sheppard, 1986), that a substantial component of connate basin fluids cannot be ruled out. The comparison of the estimated O- and H-isotope composition of Vredefort and Carbon Leader fluids (Figure 9) shows that the latter had less negative δD and $\delta^{18}O$ values. One explanation for the difference in δD value is a higher component of meteoric water (or sea water) in the Carbon Leader fluid. However, the lower $\delta^{18}O$ values in the Carbon Leader fluid might be a consequence of exchange with rocks having a generally higher $\delta^{18}O$ value (i.e. more quartz-rich) and/or at lower temperatures. In a rock-buffered system (i.e. with relatively low integrated water/rock ratio), the effect of low temperature is to lower fluid $\delta^{18}O$ value because of the increase in $\Delta_{rock\text{-}water}$. This means that is possible that the difference in isotope composition between Vredefort and the Carbon leader fluids is due to the temperature gradient from amphibolites to greenschist facies away from the Vredefort Dome.

Gold concentration and stable isotopes

The highest gold concentrations in the Witwatersrand Supergroup are typically found within the conglomeratic horizons (Barnicoat et al., 1997; Jolley et al., 2004; Frimmel et al., 2005) and the Carbon Leader Reef is no exception. Although the gold concentration in the Carbon Leader Reef varies significantly, both on a centimetre and metre-scale, horizontally and vertically between different units, the gold concentration found in the two conglomeratic units (Table 1) is orders of magnitude higher than the gold concentrations in the adjacent quartzites.

The Lower conglomerate has a significantly higher gold concentration than the Upper conglomerate, with average concentrations of 89.5 ppm and 61.5 ppm, respectively, whereas the footwall quartzite, middle quartzite and hangingwall quartzite are all relatively depleted in gold with average values of 2.9 ppm, 5.8 ppm and 1.6 ppm, respectively. Figure 10 shows a plot of $\delta^{18}O$ and δD values *vs.* gold concentration for the individual lithological units. The three quartzites show a small range between 0 ppm and 15 ppm gold, whereas the conglomerates vary significantly in gold concentration. However, the lack of correlation between $\delta^{18}O$ and δD values and gold concentration within the conglomerates suggests that external hydrothermal fluids have not been important in the processes of gold concentration.

Barnicoat et al. (1997) rejected the placer model and instead suggested that mineralization of hydrocarbon and uraninite occurred after the formation of the phyllosilicates and was then followed by gold mineralization at a later stage. It was also suggested that the distribution of this late stage hydrothermal gold was associated with thrusting during the early part of the Klipriviersberg Group. Jolley et al. (2004) suggested

that the distribution of the gold occured along small-scale shear zones and fracture swarms within the conglomerates. If the gold distribution was indeed controlled by the fabric of the conglomerate, and it is assumed that the hydrothermal fluid was of external origin, differences in $\delta^{18}O$ and δD values ought to exist between the conglomerates and the adjacent quartzites. The results of this study show that a difference does not occur, and indicate that the influence of external hydrothermal fluids on the gold concentration and distribution in the Carbon Leader Reef was limited.

Conclusion

1. The $\delta^{18}O$ values of the various rock types of the Carbon Leader Reef show a limited range and there is no correlation between $\delta^{18}O$ value and the amount of matrix present. This suggests that the detrital quartz grains and the matrix have very similar $\delta^{18}O$ values.
2. The $\delta^{18}O$ values from Carbon Leader Reef are very similar to data obtained from Witwatersrand Basin samples by Barton et al. (1992) and Vennemann et al. (1992; 1995).
3. The range in δD values of the rocks suggests that the fluid δD value was between +5 and -40‰. The ultimate origin of the fluid could be water that was incorporated in the sedimentary formations during time of deposition and later released during prograde metamorphism of the Witwatersrand sediments. There is no evidence to suggest that the fluid was from any external source.
4. There is no correlation between the oxygen and hydrogen isotope composition of the Carbon Leader Reef and the distribution and concentration of gold within the different units. This is to be expected if the gold is of placer origin. The lack of O- and H-isotope imprint from an external fluid suggests that the gold was not of hydrothermal origin. Our data are not inconsistent with the modified placer model provided the source of the fluids is internal.

Acknowledgements

We are indebted to Fayrooza Rawoot for help in the Stable Isotope laboratory. DG would like to thank the Geology Department at Tau Tona Mine, in particular to Mark Watts and Pieter Van Zyl, for numerous informative discussions. We would like to thank AngloGold Ashanti for their financial support during this work, and for permission to publish. Constructive reviews by Jay Barton and Reiner Klemd helped to improve the final version.

References

Barton, J.M., Wenner, D.B. and Hallbauer, D.K. (1992). Oxygen isotopic study of the nature and provenance of large quartz and chert clasts in gold-bearing conglomerates of South Africa. *Geology,* **20**, 1123–1126.

Barnicoat, A.C., Henderson, J.H.C., Knipe, R.J., Yardley, B.W.D., Napier, R.W., Fox, P.C., Kenyon, A.K., Muntingh, D.J., Strydom, D., Winkler, K.S., Lawrence, S.R. and Cornford, C. (1997). Hydrothermal gold mineralization in the Witwatersrand basin. *Nature*, **386**, 820–824.

Buick, I.S., Maas, R. and Gibson, R.L. (2001). Precise U-Pb titanite age constraints on the emplacement of the Bushveld Complex, South Africa. *Journal of the Geological Society of London* **158**, 3–6.

Clayton, R. N., O'Neil, J.R. and Mayeda, T.K. (1972). Oxygen isotope exchange between quartz and water. *Journal of Geophysical Research*, **77**, 3057–3067.

Craig, H. (1961). Isotopic variations in meteoric waters. *Science*, **133**, 1702–1703.

Drennan, G.R., Boiron M.-C., Cathelineau M. and Robb L.J. (1999). Characteristics of post-depositional fluids in the Witwatersrand Basin. *Mineralogy and Petrology,* **66**, 83–109.

Engelbrecht, C.J., Baumbach, G.W.S., Matthysen, J.L. and Fletcher, P. (1986). The West Wits Line. *In:* C.R. Anhaeusser and S. Maske (Editors), Mineral Deposits of South Africa, *Geological Society of South Africa*, 599–648.

Fagereng, Å., Harris, C., La Grange, M. and Stevens, G. (2008). Stable isotope study of the Archaean rocks of the Vredefort impact structure, central Kaapvaal Craton, South Africa. *Contributions to Mineralogy and Petrology,* **155**, 63–78.

Frimmel, H.E. (1994). Metamorphism of Witwatersrand gold. *Exploration and Mining Geology*, **3**, 357–370.

Frimmel, H.E (2008). Archaean atmospheric evolution: evidence from the Witwatersrand gold fields, South Africa, *Earth-Science Reviews*, **70**, 1–46.

Frimmel, H. E. and Gartz, V. H. (1997). Witwatersrand gold particle chemistry matches model of metamorphosed, hydrothermally altered placer deposit. *Mineralium Deposita*, **32**, 523–530.

Frimmel, H.E., Groves, D.I., Kirk, J., Ruitz, J., Chesley, J. and Minter, W.E.L. (2005). The Formation and Preservation of the Witwatersrand Goldfields, the World's Largest Gold Province. *Society of Economic Geologist, 100th Anniversary Volume*, 769–797.

Frimmel, H.E., Hallbauer D.K. and Gartz, V.H. (1999). Gold mobilizing fluids in the Witwatersrand basin: composition and possible sources. *Mineralogy and Petrology,* **66**, 55–81.

Frimmel, H.E. and Minter, W.E.L. (2002). Recent developments concerning the Geological History and Genesis of the Witwatersrand Gold Deposits, South Africa. *In:* R.J. Goldfarb, R.L. Nielsen (Editors), *Integrated Methods for Discovery: Global Exploration in the Twenty-First Century*. Special Publication Society of Economic Geologists, Littleton, **9**, 17–45.

Graton L. C. (1930). Hydrothermal origin of the Rand gold deposits. Part I. Testimony of the conglomerates. *Economic Geology,* **25** (supplement 3), 1–185.

Hallbauer, D. K. and Utter, T. (1977). Geochemical and morphological characteristics of gold particles from recent river deposits and the fossil placers of the Witwatersrand. *Mineralium Deposita*, **12**, 296–306.

Harris, C. and Watkins, R.T. (1990). Fluid interaction in the Witwatersrand goldfields: Oxygen isotope geochemistry of Ventersdorp-age dolerite intrusions. *South African Journal of Geology*, **93**, 611–615.

Jolley, S.J., Freeman, S.R., Barnicoat, A.C., Phillips, G.M., Knipe, R.J., Pather, A., Fox, V.P.C., Strydom, D., Birch, M.T.G., Henderson, I.H.C. and Rowland, T.W. (2004). Structural controls on Witwatersrand gold mineralization. *Journal of Structural Geology*, **26**, 1067–1086.

Karpeta, W.P. and Els, B.G., (1999). The auriferous Late Archaean Central Rand Group of South Africa: sea-level control of sedimentation? *Precambrian Research*, **97**, 191–214.

Klemd, R. (1999). A comparison of fluids causing post-depositional hydrothermal alteration in Archaean basement granitoids and the Witwatersrand Basin *Mineralogy and Petrology*, **66**,111–122

Matsuhisa, Y., Goldsmith, J.R. and Clayton, R.N. (1979). Oxygen isotopic fractionation in the system quartz-albite-anorthite-water. *Geochimica et Cosmochimica Acta*, **43**, 1131–1140.

Mellor, E. T. (1916). The conglomerates of the Witwatersrand. *Transactions of the Institute of Mining and Metallurgy,* **25**, 226–348.

Mineral Resource Statement. (2006). Unpublished. TauTona Mine Geology Department of AngloGold Ashanti Limited.

Moser D.E. (1997). Dating the shock wave and thermal imprint of the giant Vredefort impact, South Africa. *Geology,* **25**, 7–10

Mossman, D.J., Minter, W.E.L., Dutkiewicz, A.,Hallbauer, D.K., George, S.C., Hennigh, Q., Reimer, T.O. and Horscroft, F.D. (2008). The indigenous origin of Witwatersrand "carbon", *Precambrian Research,* **164**, 173–186.

O'Neil, J.R. and Taylor, H.P. (1969). Oxygen isotope equilibrium between muscovite and water. *American Mineralogist*, **52**, 1414–1437.

Phillips, G.N. and Law, J.D.M. (1994). Metamorphism of the Witwatersrand

gold fields: A review. *Ore Geology Reviews*, **9**, 1–31.

Phillips, G.N. Law, J.D.M. and Myers, R.E. (1990). The role of fluids in the evolution of the Witwatersrand Basin. *South African Journal of Geology*, **93**, 54–69.

Pretorius, D. A. (1974). Gold in the Proterozoic sediments of South Africa; systems, paradigms, and models. *Information circular*, *Economic Geology Research Unit University of the Witwatersrand, South Africa,* **87**, 2pp.

Robb, L.J. and Meyer, F.M. (1991). A contribution to recent debate concerning epigenetic versus syngenetic mineralization process in the Witwatersrand basin. *Economic Geology*, **86**, 396–401.

Sheppard, S.M.F. (1986). Characterization and isotopic variations in natural waters. *Reviews in Mineralogy*, **16**, 165–183.

Sheppard, S. M. F. and Gilg, H. A. (1996). Stable isotope geochemistry of clay minerals. *Clay Minerals*, **31**, 1–24.

Spangenberg, J. and Frimmel, H. (2001). Basin-internal derivation of hydrocarbons in the Witwatersrand basin, South Africa: evidence from bulk and molecular ^{13}C data. *Chemical Geology*, **173**, 339–355.

Stanistreet, I.G. and McCarthy, T.S. (1991). Changing tectono-sedimentary scenarios relevant to the development of the Late Archaean Witwatersrand Basin. *Journal of African Earth Sciences*, **13**, 65–81.

Suzuoki, T. and Epstein, S. (1976). hydrogen isotope fractionation between OH-bearing minerals and water. *Geochimica et Cosmochimica Acta*, **40**, 1229–1240.

Taylor H.P. (1974). The application of oxygen and hydrogen isotope studies to problems of hydrothermal alteration and ore deposition. *Economic Geology*, **69**, 843–883.

Vennemann, T.W., Kesler, S.E. and O'Neil J.R. (1992). Stable isotope compositions of quartz pebbles and their fluid inclusions as tracers of sediment provenance: implications for gold- and uranium-bearing quartz pebble conglomerates. *Geology*, **20**, 837–840.

Vennemann, T.W., Kesler, S.E., Frederickson, G.C., Minter, W.E.L. and Heine, R.R. (1995). Oxygen isotope sedimentology of gold- and uranium-bearing Witwatersrand and Huronian Supergroup quartz-pebble conglomerates. *Economic Geology*, **91**, 322–342.

Vennemann, T. W. and O'Neil, J.R. (1993). A simple and inexpensive method of hydrogen isotope and water analyses of minerals and rocks based on a zinc reagent. *Chemical Geology (Isotope Geoscience)*, **103**, 227–234.

Zhao, B., Robb, L.J., Harris, C. and Jordaan, L.J. (2006). Origin of hydrothermal fluids and gold mineralization associated with the Ventersdorp contact reef, Witwatersrand Basin, South Africa: Constraints from S, O, and H isotopes. *In:* W.U. Reimold and R.L. Gibson (Editors), Processes on the Early Earth, *Geological Society of America, Special Paper,* **405**, 333–352.

Editorial handling: L. D. Ashwal